Concentration of Small Ring Structures in Vitreous Silica from a First-Principles Analysis of the Raman Spectrum

P. Umari,[1,2] Xavier Gonze,[3] and Alfredo Pasquarello[1,2]

[1]*Institut de Théorie des Phénomènes Physiques (ITP), Ecole Polytechnique Fédérale de Lausanne (EPFL), CH-1015 Lausanne, Switzerland*

[2]*Institut Romand de Recherche Numérique en Physique des Matériaux (IRRMA), CH-1015 Lausanne, Switzerland*

[3]*Unité de Physico-Chimie et de Physique des Matériaux, Université Catholique de Louvain, B-1348 Louvain-la-Neuve, Belgium*

(Received 25 July 2002; published 13 January 2003)

Using a first-principles approach, we calculate Raman spectra for a model structure of vitreous silica. We develop a perturbational method for calculating the dielectric tensor in an ultrasoft pseudopotential scheme and obtain Raman coupling tensors by finite differences with respect to atomic displacements. For frequencies below 1000 cm^{-1}, the parallel-polarized Raman spectrum of vitreous silica is dominated by oxygen bending motions, showing a strong sensitivity to the intermediate range structure. By modeling the Raman coupling, we derive estimates for the concentrations of three- and four-membered rings from the experimental intensities of the Raman defect lines.

DOI: 10.1103/PhysRevLett.90.027401 PACS numbers: 78.30.–j, 61.43.Fs, 63.50.+x, 71.15.Mb

Raman spectroscopy is routinely used in many experimental laboratories for investigating vibrational properties of materials [1]. While Raman frequency shifts directly give access to vibrational frequencies, a meaningful interpretation of Raman cross sections necessarily relies on accurate theoretical modeling. For disordered materials, the spectrum of vibrational frequencies is continuous and the provided information is mainly contained in the distribution of Raman intensities [1]. Such information could also include *structural* properties, which are not accessible by any other experimental probe [2]. For instance, in the case of vitreous silica, the Raman spectrum shows two sharp defect lines, known as D_1 and D_2 [3,4], which have convincingly been assigned to breathing vibrations of O atoms in four- and three-membered ring structures, respectively [5–7]. The concentrations of such rings are in principle related to the intensities of the defect lines but remain elusive in the absence of a reliable description of Raman cross sections.

Theoretical approaches based on density-functional theory have proved successful in the description of Raman spectra of crystalline materials [8]. In particular, for α-quartz, calculated and measured intensities have been found to agree within an average error of 13% [9]. These methods should give results of similar accuracy for disordered systems, but their application to such cases has so far been prevented by their prohibitive computational cost. Therefore, one generally has recourse to simpler but less reliable schemes [10].

In this Letter we calculate from first principles the Raman spectra for a model structure of vitreous silica [11]. We develop a general perturbational method to calculate the dielectric tensor within a scheme based on plane-wave basis sets and ultrasoft pseudopotentials (PPs) [12,13], suitable to treat atomistic model structures of relatively large size. Raman cross sections are then obtained by finite differences with respect to atomic displacements. The calculated parallel-polarized (usually noted HH) Raman spectrum shows a strong sensitivity to O bending motions. In particular, we find a clear dependence of the Raman coupling on the Si-O-Si angle. Finally, we derive the concentrations of three- and four-membered ring structures in vitreous silica from the experimental intensities of the Raman defect lines.

In a first-order Stokes process of Raman scattering, an incoming photon of frequency ω_L and polarization $\hat{\mathbf{e}}_L$ gives an outgoing photon of frequency ω_S and polarization $\hat{\mathbf{e}}_S$ and a vibrational excitation of frequency $\omega_k = \omega_L - \omega_S$. The Raman cross section (in esu units) is given by [1]

$$\frac{d^2\sigma}{d\Omega dE} = \sum_k \frac{\omega_S^4 V}{c^4} |\hat{\mathbf{e}}_S \cdot \boldsymbol{\alpha}^k \cdot \hat{\mathbf{e}}_L|^2 \frac{\hbar}{2\omega_k} [n(\hbar\omega_k) + 1] \times \delta(E - \hbar\omega_k), \quad (1)$$

where V is the volume of the sample, c is the speed of light, E is the exchanged energy, $n(\hbar\omega)$ is the boson occupation factor, and $\boldsymbol{\alpha}^k$ is the Raman susceptibility associated to the normal mode k:

$$\alpha^k_{\mu\nu} = \sqrt{V} \sum_{I\gamma} \frac{\partial \chi_{\mu\nu}}{\partial R_{I\gamma}} \xi^k_{I\gamma} / \sqrt{M_I}, \quad (2)$$

where $\chi_{\mu\nu}$ is the dielectric polarizability tensor, $\boldsymbol{\xi}^k_I$ are the vibrational eigenmodes, M_I is the atomic mass, and $\mathbf{R}_I$ is the atomic position of atom I. Hence, in addition to the vibrational frequencies and eigenmodes, the calculation of Raman cross sections requires the derivatives of the polarizability tensor with respect to atomic displacements ($\partial\boldsymbol{\chi}/\partial\mathbf{R}$).

We determined the polarizability tensor within variational density-functional perturbation theory [14,15]. To

treat disordered systems of large size including first-row elements, we extended the scheme developed in Ref. [15] for norm-conserving PPs to the case of ultrasoft PPs [12]. At variance with previous treatments of the polarizability tensor [8,15], the perturbation due to an electric field is first considered at the level of the *all-electron* Hamiltonian. The perturbation scheme for ultrasoft pseudopotentials is then derived by transforming the all-electron valence wave functions (zero- and first-order) into pseudo ones [12,16,17]. This scheme, which also applies to the projector augmented-wave method [16], gives perturbative expressions in a straightforward way [18]. For small molecules, such as H_2O, NH_3, and CH_4, we obtained Raman intensities in excellent agreement with documented results [19–21]. For instance, for H_2O, we obtained intensities of 0.739, 119, 25.6 $\text{Å}^4 \cdot \text{amu}^{-1}$ for modes of increasing frequency, to be compared with all-electron results of 0.632, 115, 24.8 $\text{Å}^4 \cdot \text{amu}^{-1}$ [19] and experimental results of 0.9 ± 2, 108 ± 14, 19.2 ± 2.1 $\text{Å}^4 \cdot \text{amu}^{-1}$ [21].

In our study of vitreous silica, we considered at first a model structure consisting of a network of corner-sharing tetrahedra, generated by first-principles molecular dynamics [11]. This model structure contains 72 atoms in a periodically repeated cubic cell, at the experimental density (2.20 g/cm^3). The inelastic neutron scattering and infrared absorption spectra were previously calculated for the same model structure and found in good agreement with experiment [22,23]. The choice of this model structure was motivated by the opportunity of obtaining theoretical spectra associated to the three principal vibrational spectroscopies for the same atomic structure.

The polarizability was calculated within the local density approximation to density-functional theory. We used a norm-conserving PP for Si [24] and an ultrasoft PP for O [12]. The electronic parameters for the calculation of the polarizability were set as in Ref. [22], where the vibrational frequencies ω_k and eigenmodes $\boldsymbol{\xi}_I^k$ were acquired. The derivatives $\partial\boldsymbol{\chi}/\partial\mathbf{R}$ were obtained for every atom in the model by taking finite differences of the polarizability tensors calculated as described above. We used atomic displacements of ± 0.07 bohr, in a regime in which the polarizability shows a linear dependence.

Raman spectra of disordered materials are usually recorded in configurations in which the polarizations of incoming and outgoing photons are either parallel (HH) or perpendicular (HV) [1]. We calculated HH and HV spectra by taking appropriate orientational averages [1]. Theoretical and experimental spectra [5] are compared in Fig. 1. Since the experimental spectra are given on a relative scale, we rescaled the theoretical ones by a constant factor to match the integrated intensity of the experimental HH spectrum. The overall comparison between theory and experiment is not impressive. A fair agreement is found for the location of the principal peaks and for the average ratio between the intensities of the HH and HV spectra. However, significant differences occur in the HH spectrum for frequencies ranging from 300 to 700 cm^{-1}, precisely where the D_1 and D_2 lines appear. In the calculated HH spectrum, the intensity of the large peak at $\sim$450 cm^{-1} is underestimated while the D_2 line is more intense than in the experiment. This shift of intensity towards the D_2 line is consistent with the occurrence of a high concentration of three-membered rings in our model structure [6], for which as much as 30% of the O atoms belong to such rings. This suggests that the differences between theory and experiment in Fig. 1 result from a different description of the intermediate range order in the model structure rather than from an inaccurate determination of the Raman intensities. This interpretation is supported by the good agreement between first-principles and experimental intensities found for α-quartz [9].

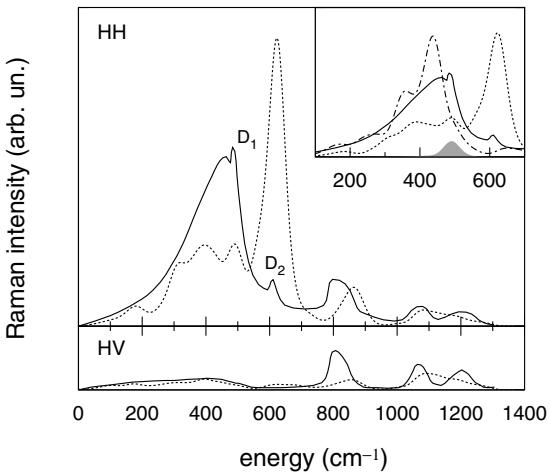

FIG. 1. Calculated (dotted line) and measured [5] (solid line) reduced HH and HV Raman spectra of vitreous silica. The calculated spectra are scaled to match the integrated intensity of the experimental HH spectrum. The integrated Raman intensity under the theoretical HH curve is 2.01×10^{-7} $\text{bohr}^{-2} \cdot \text{amu}^{-1}$. For clarity, the curves in the lower panel are magnified by a factor of 2. A Gaussian broadening is used (22 cm^{-1}). Inset: HH Raman spectrum for the second model structure defined in the text (dot-dashed line) compared to experiment (solid line) and to the initial model structure (dotted line). The contribution from the breathing vibration in the four-membered ring is shaded.

In order to define the properties that an improved model structure of vitreous silica should satisfy, we further analyze the sensitivity of the HH Raman spectrum to the intermediate range order. By considering the contribution from O and Si atoms separately, we found that the HH Raman spectrum in the frequency region below 1000 cm^{-1} almost exclusively arises from the coupling to O motions. We then analyzed the tensors $\partial\boldsymbol{\chi}/\partial\mathbf{R}$ associated to O atoms in terms of a local basis set. This analysis shows that the intensity is principally given by the fully isotropic components resulting, for every O atom I, from bending motions along the bisector direction $\hat{\mathbf{b}}_I$ of the Si-O-Si bond angle. The associated Raman coupling

can thus be expressed in terms of a scalar coupling factor,

$$f_I = \frac{1}{3} V \,\mathrm{Tr} \sum_{\gamma} \frac{\partial \chi_{\alpha\beta}}{\partial R_{I\gamma}} b_{I\gamma}, \tag{3}$$

normalized to be volume independent. The HH spectrum calculated on this basis is confronted in Fig. 2 with the one obtained with the full coupling tensors. This comparison shows that the f_I provide an excellent description of the HH spectrum for frequencies below 1000 cm^{-1}. Note that the f_I do not contribute to the HV spectrum which arises solely from nonisotropic components [1]. This explains why the HV spectrum does not show defect lines.

The coupling factors f_I associated to the O atoms in the model structure show a clear correlation with the Si-O-Si bond angle θ_I (Fig. 2, inset). This correlation is consistent with the relation

$$f_I = (\alpha/3)\cos(\theta_I/2), \tag{4}$$

predicted by the bond polarizability model for a system of regular tetrahedral units [9]. Using the data in Fig. 2, we derived an optimal value of 46.5 bohr^2 for α. The coupling factors calculated by first principles for α-quartz and for a set of cristobalite structures [9] are also well described by (4) with the same value of α (Fig. 2, inset).

The modeling scheme introduced above provides us with a viable framework for deriving the concentration of three- and four-membered rings from the *experimental* HH Raman spectrum. We assumed that the contribution from O bending motions accounts for the entire Raman spectrum up to 1000 cm^{-1}, via the coupling factors f_I. For the hypothetical case of a constant coupling factor, the intensity can be shown to be strictly proportional

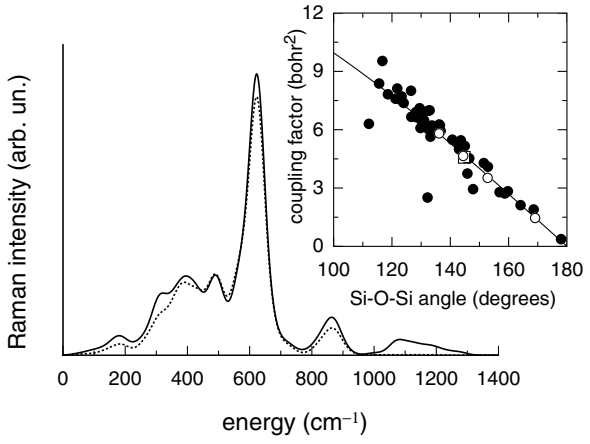

FIG. 2. Full HH spectrum (solid line) compared with the one obtained with coupling tensors in which only the fully isotropic components resulting from O bending motions are retained (dotted line). Inset: coupling factor f_I vs the Si-O-Si angle θ for all O atoms in our model structure of vitreous silica (disks), in α-quartz (square), and in a set of cristobalite structures (circles). The correlation is well described by Eq. (4) with $\alpha = 46.5$ bohr^2 (solid line).

to the number of O atoms, because of the isotropic nature of the adopted coupling. Under such an assumption, the concentration of three- and four-membered rings has tentatively been estimated to be about 1% [5,25]. In the present study, an estimate is provided which accounts for the dependence of the coupling factor on the Si-O-Si angle. On the basis of (4), we estimated this effect by considering the average Si-O-Si angle in three- ($\theta_{3R} \approx 128°$ [6]), and in four-membered rings ($\theta_{4R} \approx 136°$ [6]) with respect to that in vitreous silica ($\langle\theta\rangle \approx 151°$ [26]). The ratios between the intensities of each of the defect lines and the background are therefore enhanced with respect to the concentration of O atoms in the small rings. We derived enhancement factors of $\cos^2(\theta_{3R}/2)/\cos^2(\langle\theta\rangle/2) = 3.1$ and $\cos^2(\theta_{4R}/2)/\cos^2(\langle\theta\rangle/2) = 2.2$ for the D_2 and D_1 lines, respectively. Using these enhancement factors and the experimental ratios between the intensities of the defect lines and the background, we obtained that 0.22% and 0.36% of the O atoms are found in three- and four-membered rings, respectively, (Table I). We stress that these results directly follow from the dependence on the Si-O-Si angle in (4) and do *not* depend on the specificity of our model structure or on the value of α.

The estimated concentrations of O atoms in small rings differ significantly from those in our model structure (31% in three- and 17% in four-membered rings) [6], most likely as a consequence of the high cooling rate used in the first-principles generation procedure [11]. To verify that a better description of intermediate range order results in an improved accord between calculated and measured Raman spectra, we then considered a second model structure. From an extended set of 72-atom model structures generated by classical molecular dynamics [31], we selected the one with the lowest amount of small rings. The selected structure contains a single four-membered ring and no three-membered rings. The intermediate range order of this model structure is characterized by an average Si-O-Si angle of 152°, close to the experimental estimate of 151° [26] and significantly different than for the model structure used initially (137°). As for the initial model structure, we relaxed the atomic

TABLE I. Oxygen concentrations in three- and four-membered rings as derived from the *experimental* HH Raman spectrum, compared to estimates from classical molecular dynamics (MD) [27,29,30]. In parentheses, we give an upper bound as derived from the spread of intensities in the model structures. The O concentrations from Refs. [29,30] are derived from the ring statistics [27]. The values from Ref. [30] correspond to the lowest cooling rate.

		MD simulations	
	Present	Ref. [29]	Ref. [30]
O in threefold rings	0.22% (0.26%)	3%	6%
O in fourfold rings	0.36% (1.0%)	26%	36%

positions and calculated the vibrational frequencies and eigenmodes within a first-principles scheme. For the range of frequencies dominated by O bending motions, we obtained the associated HH Raman spectrum (Fig. 1, inset) using the coupling factors f_I as given by (4). The calculated spectrum for the second model structure noticeably improves the agreement between theory and experiment. The peak at $\sim 440\ \mathrm{cm}^{-1}$ in the calculated spectrum agrees well, both in intensity and location, with the principal experimental peak at $\sim 450\ \mathrm{cm}^{-1}$. The theoretical spectrum does not show any feature in correspondence of the D_2 line, in accord with the absence of three-membered rings. The contribution from the breathing vibration in the four-membered ring gives a peak at $490\ \mathrm{cm}^{-1}$ [32] in excellent agreement with the D_1 line at $495\ \mathrm{cm}^{-1}$ [5].

To characterize the structure of vitreous silica beyond the short-range order, the ring-size statistics has emerged as a useful theoretical concept [28]. However, it has so far not been possible to provide any experimental data describing this statistics. Our results for the O concentrations trivially translate into amounts of three- and four-membered rings [27], providing the first estimate of this kind based on an experimental Raman spectrum. We note that the atomic structures obtained with classical molecular dynamics simulations [27,29,30] exhibit too large concentrations of small ring structures (Table I), most likely as a result of excessively high cooling rates.

In conclusion, we introduced a density-functional scheme for the calculation of Raman spectra of disordered materials. Applied to vitreous silica, we found that the HH Raman spectrum is strongly sensitive to intermediate range order, through the dominating coupling to O bending motions. The prominent role of O bending motions suggests that also in the case of other oxide glasses the Raman spectra could similarly reveal intermediate range structural properties, which would otherwise remain mostly inaccessible.

We thank A. Bongiorno for providing us with one of the model structures used in Ref. [31]. P. U. and A. P. acknowledge support from the Swiss National Science Foundation (Grants No. 21-55450.98 and No. 620-57850.99) and the Swiss Center for Scientific Computing. X. G. acknowledges support from the Belgian National Science Foundation, the "Communauté française de Belgique (A.R.C.—intéraction électro-vibration dans les nanostructures)," and the PAI/IUAP P5 Physics of nanostructures.

[1] *Light Scattering in Solids II*, edited by M. Cardona and G. Güntherodt (Springer-Verlag, Berlin, 1982).
[2] S. R. Elliott, *Physics of Amorphous Materials* (Longman Scientific & Technical, Harlow, Essex, 1990), 2nd ed.; Nature (London) **354**, 445 (1991).
[3] R. H. Stolen, J. T. Krause, and C. R. Kurkjian, Discuss. Faraday Soc. **50**, 103 (1971).
[4] F. L. Galeener and G. Lukovsky, Phys. Rev. Lett. **37**, 1474 (1976).
[5] F. L. Galeener, Solid State Commun. **44**, 1037 (1982).
[6] A. Pasquarello and R. Car, Phys. Rev. Lett. **80**, 5145 (1998).
[7] Closed paths containing n Si-O segments are referred to as n-membered rings.
[8] S. Baroni *et al.*, Rev. Mod. Phys. **73**, 515 (2001); E. T. Heyen *et al.*, Phys. Rev. Lett. **65**, 3048 (1990); P. Puschnig *et al.*, Phys. Rev. B **64**, 024519 (2001); C. Ambrosch-Draxl *et al.*, Phys. Rev. B **65**, 064501 (2002).
[9] P. Umari, A. Pasquarello, and A. Dal Corso, Phys. Rev. B **63**, 094305 (2001).
[10] R. Shuker and R. W. Gammon, Phys. Rev. Lett. **25**, 222 (1970); R. J. Bell and D. C. Hibbins-Butler, J. Phys. C **9**, 2955 (1976); P. Umari and A. Pasquarello, Physica (Amsterdam) **316B–317B**, 572 (2002).
[11] J. Sarnthein, A. Pasquarello, and R. Car, Phys. Rev. Lett. **74**, 4682 (1995); Phys. Rev. B 52, 12 690 (1995).
[12] D. Vanderbilt, Phys. Rev. B **41**, 7892 (1990).
[13] A. Pasquarello *et al.*, Phys. Rev. Lett. **69**, 1982 (1992); K. Laasonen *et al.*, Phys. Rev. B **47**, 10 142 (1993).
[14] X. Gonze, D. C. Allan, and M. P. Teter, Phys. Rev. Lett. **68**, 3603 (1992).
[15] X. Gonze, Phys. Rev. B **55**, 10 337 (1997).
[16] P. E. Blöchl, Phys. Rev. B **50**, 17 953 (1994).
[17] B. Hetényi *et al.*, J. Chem. Phys. **115**, 5791 (2001).
[18] P. Umari, X. Gonze, and A. Pasquarello (unpublished).
[19] D. Porezag and M. R. Pederson, Phys. Rev. B **54**, 7830 (1996).
[20] A. Stirling, J. Chem. Phys. **104**, 1254 (1996).
[21] W. F. Murphy, Mol. Phys. **33**, 1701 (1977); **36**, 727 (1978).
[22] J. Sarnthein, A. Pasquarello, and R. Car, Science **275**, 1925 (1997); A. Pasquarello, J. Sarnthein, and R. Car, Phys. Rev. B **57**, 14 133 (1998).
[23] A. Pasquarello and R. Car, Phys. Rev. Lett. **79**, 1766 (1997).
[24] G. B. Bachelet, D. R. Hamann, and M. Schlüter, Phys. Rev. B **26**, 4199 (1982).
[25] J. C. Mikkelsen, Jr. and F. L. Galeener, J. Non-Cryst. Solids **37**, 71 (1980).
[26] F. Mauri *et al.*, Phys. Rev. B **62**, R4786 (2000).
[27] The values for three- and four-membered rings in the ring statistics (defined by shortest path analysis [28]) are obtained by multiplying the respective O concentrations by 2. We assumed isolated rings.
[28] S. V. King, Nature (London) **213**, 1112 (1967).
[29] J. P. Rino *et al.*, Phys. Rev. B **47**, 3053 (1993).
[30] K. Vollmayr, W. Kob, and K. Binder, Phys. Rev. B **54**, 15 808 (1996); K. Vollmayr and W. Kob, Ber. Bunsen-Ges. Phys. Chem. **100**, 1399 (1996).
[31] A. Bongiorno and A. Pasquarello, Phys. Rev. Lett. **88**, 125901 (2002).
[32] This peak does not show up in the calculated spectrum because its width is overestimated as a result of the limited relaxation allowed in a 72-atom model structure [6].